

Electro-mechanical Casimir effect

Mikel Sanz,^{1,*} Witlef Wiczorek,² Simon Gröblacher,³ and Enrique Solano^{1,4,5}

¹*Department of Physical Chemistry, University of the Basque Country UPV/EHU, Apartado 644, E-48080 Bilbao, Spain*

²*Microtechnology and Nanoscience, Chalmers University of Technology, Kemivägen 9, SE-41296 Göteborg, Sweden*

³*Kavli Institute of Nanoscience, Delft University of Technology, Lorentzweg 1, 2628CJ Delft, The Netherlands*

⁴*IKERBASQUE, Basque Foundation for Science, Maria Diaz de Haro 3, E-48013 Bilbao, Spain*

⁵*Department of Physics, Shanghai University, 200444 Shanghai, People's Republic of China*

The dynamical Casimir effect is an intriguing phenomenon in which photons are generated from vacuum due to a non-adiabatic change in some boundary conditions. In particular, it connects the motion of an accelerated mechanical mirror to the generation of photons. While pioneering experiments demonstrating this effect exist, a conclusive measurement involving a mechanical resonator is still missing. We show that a hybrid system consisting of a piezoelectric mechanical resonator coupled to a superconducting cavity may allow to electro-mechanically generate measurable photons from vacuum, intrinsically associated to the dynamical Casimir effect. Such an experiment may be achieved with current technology, based on film bulk acoustic resonators directly coupled to a superconducting cavity. Our results predict a measurable photon generation, which can be further increased through additional improvements such as using superconducting metamaterials.

Introduction.—Quantum mechanics predicts that virtual particles can emerge from vacuum. This phenomenon, known as quantum fluctuations, is a cornerstone to explaining key effects in nature, ranging from the anomalous magnetic moment of the electron [1], to the enhancement in quantum transport phenomena [2], and the Lamb shift of atomic spectra [3]. Another paramount example is the Casimir effect that results from a force between two separated conducting plates. This force is mediated by vacuum due to a reduction of the density of electromagnetic modes as a consequence of the constraints imposed by the boundary conditions [4–6]. This results in a lower vacuum radiation pressure between the plates compared to outside and, consequently, an attractive force between the mirrors. G. T. Moore [7] suggested the existence of a kinetic analogue to this phenomenon, known as the dynamical Casimir effect (DCE). This effect, based on the fact that a moving mirror modifies the mode structure of the electromagnetic vacuum dynamically, is the result of a mismatch of vacuum modes in time. Indeed, if the velocity of a mirror is much smaller than the speed of light, $v \ll c$, then no excitations emerge out of the vacuum, since the electromagnetic modes adiabatically adapt to the changes. However, if the mirror experiences relativistic motion, these changes occur non-adiabatically. Hence, the vacuum state of the electromagnetic field can be excited by taking energy from the moving mirror, resulting in the generation of real photons.

A version of the DCE has recently been demonstrated with superconducting circuits by moving the electric boundary conditions instead of the center of mass of the mirror [8]. In a similar experiment, photons were created by modulating the effective speed of light [9] making use of a superconducting metamaterial. Additionally, relevant applications of these experiments, such as a robust generation of multi-partite quantum correlations [10, 11], were proposed, highlighting the potential of this effect beyond its fundamental interest. However, no experiment to date has succeeded in generating

photons out of vacuum using a moving mechanical object in the spirit of the original DCE proposal. It has indeed even been suggested that, due to the large stress generated on any macroscopic material moving with relativistic speed, such an experiment might actually be impossible [12].

In this letter, we propose an experiment consisting of a mechanical resonator that is directly coupled to a high impedance superconducting cavity, as depicted in Fig. 1 in order to create a measurable rate of photons created via the DCE. Our calculations make use of the recent advances in mechanical oscillators based on film bulk acoustic resonators (FBAR) technology using thin films of Al-AlN-Al [15]. The presence of the cavity allows for a resonant enhancement of the photon rate which surpasses the radiation from a single mirror by several orders of magnitude [13]. We study the minimally required conditions to observe a stable flux of photons resulting from the electro-mechanically amplified quantum vacuum, concluding that such a measurement is feasible with current technology. Finally, we propose technical improvements to further enhance the photon mechanical production. Our work also paves the way to experimentally test other fundamental relativistic effects with mechanical resonators, such as the Unruh effect or the Hawking radiation [14].

Proposed implementation.—The proposed setup consists of a piezoelectric FBAR resonator with resonance frequency $\Omega/2\pi = 4.20$ GHz coupled to a superconducting cavity with length $d = 33$ mm, which is capacitively coupled to a semi-infinite transmission line, as shown in Fig. 1. We have chosen values that closely follow the parameters from Ref. [15], for details see Appendix C. An AC voltage is applied to the superconducting plates of the mechanical resonator. This voltage drive has two effects: (i) The piezoelectric material of the FBAR converts the AC voltage into mechanical contraction or expansion, which essentially leads to a change of the length of the superconducting cavity; (ii) The voltage drive leads to a change in the potential of the cavity's boundary. Both effects lead to a production of DCE photons.

FBAR modelling.—We make use of the modified van Dyke-Butterworth model to construct the equivalent lumped-element circuit representation of the FBAR [16, 17]. This cir-

* mikel.sanz@ehu.es

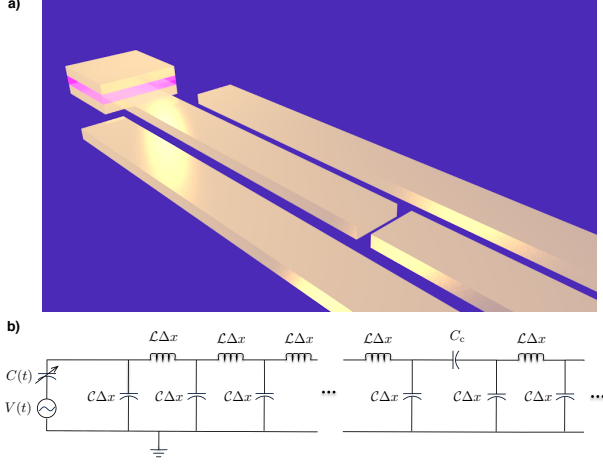


FIG. 1. Scheme of the coupling between the superconducting cavity and the FBAR. (a) Artistic view representing an FBAR, a resonator composed of two superconducting layers sandwiching a piezoelectric material, terminating one side of a superconducting cavity which is capacitively coupled to a semi-infinite transmission line and (b) equivalent circuit, which is composed of the mechanical resonator and the superconducting cavity. We have employed the modified van Dyke-Butterworth model to provide the equivalent lumped-element circuit representation of the FBAR and model the cavity as an infinite set of LC circuits which will be afterwards capacitively coupled to a semi-infinite waveguide.

circuit contains two parallel branches. The first one consists of a mechanical capacitance C_m , mechanical inductance L_m and a resistor R_m modeling the mechanical dissipation connected in series, while the second one contains a resistor R_0 taking into account the dielectric loss and, crucially, a geometrical capacitance $C(t)$, which slightly changes in time when an AC voltage is applied to the plates of the FBAR. Composing the impedances for both branches, Z_m and Z_0 , it is straightforward to prove that the total impedance $Z \approx Z_0$, which, to first order, can be reduced to $C(t)$, as depicted in Fig. 4 of Appendix B 2.

Let us estimate the change in the capacitance $C(t)$ when an AC voltage is applied to the electrodes. An AC voltage with an amplitude V_{pp} at the resonance frequency of the mechanical resonator results in a change of the inter-plate distance $\Delta x(V) \approx 1.7 \cdot V \text{ nm/V}$ (see Appendix A). Crucially, the piezoelectric effect is enhanced by the mechanical quality factor of the FBAR. For a voltage of $V_{pp} = 500 \mu\text{V}$ we get $\Delta x = 8.5 \cdot 10^{-13} \text{m}$, which is much smaller than the thickness t_{AIN} of the piezoelectric layer. Thus, we model the resulting mechanical contraction and expansion as harmonic. The time-varying capacitance is then given as $C(t) = \frac{\epsilon_{\text{AIN}} A}{d(t)} = \frac{\epsilon_{\text{AIN}} A}{t_{\text{AIN}} + \Delta x \cos(\Omega t)}$. We expand $C(t)$ for $\Delta x \ll t_{\text{AIN}}$ and finally obtain $C(t) \approx C_0 + C_0 \frac{\Delta x}{t_{\text{AIN}}} \cos(\Omega t)$ with $C_0 = \frac{\epsilon_{\text{AIN}} A}{t_{\text{AIN}}}$ and $\Delta C \approx C_0 \frac{\Delta x}{t_{\text{AIN}}}$.

Lumped-element circuit model.—The Lagrangian describing the circuit of the FBAR connected to an open transmission line (without the coupling capacitor shown in Fig. 1) can be

written as

$$L = \sum_{i=0}^{\infty} \left[\frac{\delta x C}{2} \dot{\Phi}_{i+1}^2 - \frac{1}{2\delta x \mathcal{L}} (\Phi_{i+1} - \Phi_i)^2 \right] + \frac{1}{2} C(t) (\dot{\Phi}_0 - \dot{\Phi}_v)^2 + \frac{1}{2} C_g \dot{\Phi}_0^2. \quad (1)$$

Here, C and \mathcal{L} are the capacitance and inductance of the transmission line per unit length, respectively, C_g is the capacitive coupling of the FBAR to ground, which we will discard in our analysis as it is much smaller than any other quantity involved, and Φ_i is the node flux. In the continuous limit, the equation of motion corresponding to $i = 0$ is given by

$$C(t) \ddot{\Phi}(0, t) + \dot{C}(t) \dot{\Phi}(0, t) - \frac{1}{\mathcal{L}} \frac{\partial \Phi(x, t)}{\partial x} \Big|_{x=0} = F(t), \quad (2)$$

with $F(t) = \frac{d}{dt}(\theta(t)C(t)V(t))$ being the electro-mechanical source term, and $\theta(t)$ is the Heaviside step function. In order to solve it, we follow a similar approach to Ref. [12] and expand the field in the Fourier components

$$\Phi(x, t) = \sqrt{\frac{\hbar Z_0}{4\pi}} \int_0^{\infty} d\omega \frac{1}{\sqrt{\omega}} \left[a_{\text{in}}(\omega) e^{-i(\omega t - k_\omega x)} + a_{\text{out}}(\omega) e^{-i(\omega t + k_\omega x)} + H.c. \right].$$

Eq. (2) can now be written as

$$\int_0^{\infty} d\omega \sqrt{\frac{\hbar Z_0}{4\pi|\omega|}} \left[\left(-\omega^2 C(t) - i\omega \dot{C}(t) - \frac{ik_\omega}{\mathcal{L}} \right) a_{\text{in}}(\omega) e^{-i\omega t} + \left(-\omega^2 C(t) - i\omega \dot{C}(t) + \frac{ik_\omega}{\mathcal{L}} \right) a_{\text{out}}(\omega) e^{-i\omega t} + H.c. \right] = F(t).$$

By integrating over $\int_{-\infty}^{\infty} dt \sqrt{|\omega'|} e^{i\omega' t}$, we can see that in the case of a static capacitor, it behaves as a mirror placed at $x = -L_{\text{eff}} \approx \frac{C_0}{\mathcal{L}}$, such that the effective length of the resonator is $d_{\text{eff}} = d + L_{\text{eff}}$.

For a harmonically oscillating capacitor with a voltage source at the same frequency but with a phase difference, we can write $C(t) = C_0 + \Delta C \cos(\Omega t)$ and $V(t) = V_{pp} \cos(\Omega t + \phi)$. Resonances emerge due to the inelastic interaction of the photons with the oscillating mirror, and the incoming modes $a_{\text{in}}(\omega)$ with frequency ω are scattered elastically as $a_{\text{out}}(\omega)$ and inelastically as $a_{\text{out}}(\omega + \Omega)$, $a_{\text{out}}(\omega + 2\Omega)$, Keeping only the first inelastic resonances, as higher resonances have higher orders in ΔC , and assuming that $0 < \omega \leq \Omega$, which is natural since the condition for the rotating wave approximation holds around $\Omega \approx 2\omega'$, the output mode is given by

$$a_{\text{out}}(\omega, L_{\text{eff}}) = h(\omega, \Omega) + a_{\text{in}}(\omega, L_{\text{eff}}) + S(\omega, \Omega + \omega) a_{\text{in}}(\Omega + \omega, L_{\text{eff}}) + S(\omega, \Omega - \omega) a_{\text{in}}^\dagger(\Omega - \omega, L_{\text{eff}}). \quad (3)$$

Here the operators a_{in} and a_{out} are defined in the displaced position $x = L_{\text{eff}}$, $h(\omega, \Omega)$ is the identity in operator space as we have treated the source classically, and

$$S(\omega', \omega'') = -i\Delta C Z_0 \sqrt{|\omega'| |\omega''|} \theta(\omega') \theta(\omega''), \quad (4)$$

$$h(\omega, \Omega) = -i\sqrt{\frac{4\pi Z_0}{\hbar\omega}} \mathcal{F}(\omega, \Omega), \quad (5)$$

with $\mathcal{F}(\omega, \Omega) = (2\pi)^{-1/2} \int_{-\infty}^{\infty} dt F(t) e^{i\omega t}$ being the Fourier transform of $F(t)$. The coefficient in Eq. (4) can also be written using $\Delta C \approx C_0 \frac{\Delta x}{t_{\text{AIN}}}$, with $Z_0 \approx 55 \Omega$ and C_0 the Casimir coupling capacitance.

Electro-mechanical DCE photon rate.—The aforementioned result describes an oscillatory mirror coupled to a one-dimensional open transmission line. The photon production due to the change in the boundary conditions can be dramatically increased by introducing a cavity with a well chosen resonance condition, as shown for example in Ref. [13]. In order to realize this, we will introduce a capacitor at a distance d of the FBAR, as depicted in Fig. 1. We redefine the origin of the coordinates in the coupling capacitance between the cavity and the line and hence the harmonic mirror is placed at $x = d_{\text{eff}} = d + L_{\text{eff}}$, with d the length of the cavity for a static mirror. Therefore, the natural frequency of the resonator is $\omega_0/2\pi = v/d_{\text{eff}}$. The input-output relations connecting the fields inside the cavity $\{a_{\text{in}}, a_{\text{out}}\}$ to fields in the transmission line $\{b_{\text{in}}, b_{\text{out}}\}$ are given by

$$\begin{pmatrix} a_{\text{in}}(\omega, 0) \\ a_{\text{out}}(\omega, 0) \end{pmatrix} = \begin{pmatrix} \bar{\alpha}_\omega & \beta_\omega \\ \beta_\omega & \alpha_\omega \end{pmatrix} \begin{pmatrix} b_{\text{in}}(\omega, 0) \\ b_{\text{out}}(\omega, 0) \end{pmatrix}, \quad (6)$$

with $\alpha_\omega = 1 + \frac{i\omega_c}{2\omega}$, $\beta_\omega = \frac{i\omega_c}{2\omega}$ and $\omega_c = \frac{1}{C_c Z_0}$. Notice that ω_c is a measure of how large the coupling of the resonator to the line is. Indeed, for $\omega_c \gg \omega$ it is completely decoupled, while $\omega_c = 0$ means that there is no cavity. Equation (6) holds for $x = 0$ [12], but as we want to connect the fields in the line with the reflected fields on the oscillating mirror, we must displace the cavity fields to $x = d_{\text{eff}}$ by using the matrix $\text{diag}(e^{ik_\omega d_{\text{eff}}}, e^{-ik_\omega d_{\text{eff}}})$. In order to compute the reflection coefficient $R_{\text{res}}(\omega)$, we can consider that the inelastic scattering process is absent and that only the reflection-transmission process remains, so $a_{\text{in}}(\omega, d_{\text{eff}}) = a_{\text{out}}(\omega, d_{\text{eff}})$. Under this condition, we get

$$R_{\text{res}}(\omega) = \frac{1 + (1 + \frac{2i\omega}{\omega_c}) e^{2ik_\omega d_{\text{eff}}}}{(1 - \frac{2i\omega}{\omega_c}) + e^{2ik_\omega d_{\text{eff}}}}. \quad (7)$$

Similarly, we also want to study the mode structure of the resonator. This information is encoded in the function A_{res} , defined as $a_{\text{out}}(\omega, d_{\text{eff}}) = A_{\text{res}}(\omega) b_{\text{in}}(\omega, 0)$, as it contains the response of the resonator to any input signal coming from the line,

$$A_{\text{res}}(\omega) = \frac{(\frac{2i\omega}{\omega_c}) e^{ik_\omega d_{\text{eff}}}}{(1 - \frac{2i\omega}{\omega_c}) + e^{-2ik_\omega d_{\text{eff}}}}. \quad (8)$$

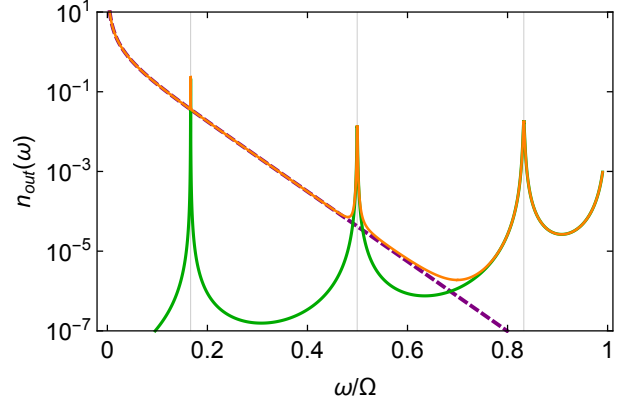


FIG. 2. (Color online) Electro-mechanical photon production. The orange (light gray) line depicts the total number of photons in the open transmission line that originate from the DCE effect and thermal radiation. The green (dark gray) line shows the photons only generated via the electro-mechanical DCE effect, whereas the purple (dashed) line shows the thermal contribution. The vertical gray lines depict the resonances of the superconducting cavity.

The resonance frequencies can be deduced from the denominator of Eq. (8) and, as shown in Ref. [12], they are approximately the solutions of the transcendental equation $\tan(2\pi\omega/\omega_0) = \omega_c/\omega$. The outgoing mode in the open transmission line in the presence of a driven FBAR, keeping only the first order of $S(\omega', \omega'')$, reads

$$\begin{aligned} b_{\text{out}}(\omega) &= h_{\text{res}}(\omega, \Omega) + R_{\text{res}}(\omega) b_{\text{in}}(\omega) \\ &+ S_1^{\text{res}}(\omega, \Omega + \omega) b_{\text{in}}(\Omega + \omega) \\ &+ \bar{S}_2^{\text{res}}(\omega, \Omega - \omega) b_{\text{in}}^\dagger(\Omega - \omega), \end{aligned} \quad (9)$$

with

$$\begin{aligned} h_{\text{res}}(\omega, \Omega) &= h(\omega, \Omega) \left[\left(1 - \frac{2i\omega}{\omega_c}\right) + e^{-2ik_\omega d_{\text{eff}}} \right]^{-1} \\ S_1^{\text{res}}(\omega', \omega'') &= S(\omega', \omega'') A(|\omega'|) A(|\omega''|) \\ S_2^{\text{res}}(\omega', \omega'') &= S(\omega', \omega'') \bar{A}(|\omega'|) A(|\omega''|). \end{aligned}$$

For an initial thermal state, the mean photon number $n_{\text{out}}(\omega) = \langle b_{\text{out}}^\dagger(\omega) b_{\text{out}}(\omega) \rangle_T$ is given by

$$\begin{aligned} n_{\text{out}}(\omega) &= |R_{\text{res}}(\omega)|^2 n_{\text{in}}(\omega) + |S_1^{\text{res}}(\omega, \Omega + \omega)|^2 n_{\text{in}}(\Omega + \omega) \\ &+ |S_2^{\text{res}}(\omega, \Omega - \omega)|^2 [1 + n_{\text{in}}(\Omega - \omega)] \\ &+ |h_{\text{res}}(\omega, \Omega)|^2, \end{aligned} \quad (10)$$

where $n_{\text{in}}(\omega) = \left[\exp(\frac{\hbar\omega}{k_B T}) - 1 \right]^{-1}$ is the thermal photon occupation at temperature T . The photon production of electro-mechanical Casimir origin is given by the term $|S_2^{\text{res}}(\omega, \Omega - \omega)|^2 + |h_{\text{res}}(\omega, \Omega)|^2$. The total mean photon number $n_{\text{out}}(\omega)$ is plotted in Fig. 2. For $\omega/\Omega = 1/2$ we see that the Casimir photon production is of the order of 10^{-2} photons/s for a driving voltage of $V_{\text{pp}} = 5 \times 10^{-4}$ V. Such a rate should easily be measurable with current technology [20, 21].

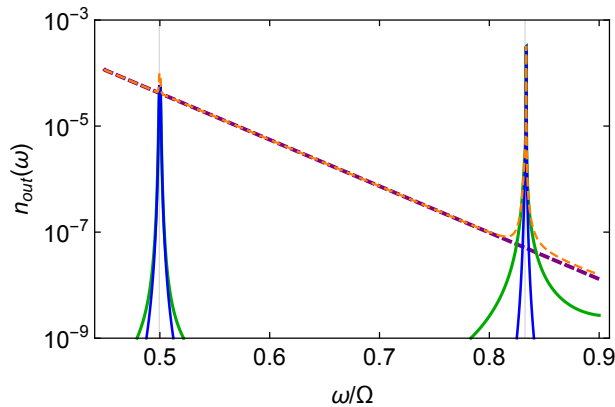


FIG. 3. (Color online) Purely mechanical photon production for an improved device. The orange, dashed (light gray, dashed) line depicts the total number of photons in the open transmission line that originate from the DCE effect and thermal radiation. The green (dark gray) line shows the photons only generated via the electro-mechanical DCE effect. the blue (gray) line shows the photons only generated via the mechanical part of the DCE effect. The purple (dashed) line shows the thermal contribution. The vertical gray lines depict the resonances of the superconducting cavity.

The DCE part of the total photon number is well above the thermal photon noise floor.

The non-adiabatic change in the boundary conditions is of electro-mechanical nature, as the voltage driving the FBAR also produces a change in the potential of the boundary, in addition to the mechanical movement of the plate. Even though it can not be measured, one may wonder about the ratio of the photon production which is purely due to the mechanical movement. In order to calculate electrically generated photons, we consider the situation in which the piezoelectric material is removed, i.e., $\Delta C = 0$, while the voltage source is still connected. By subtracting this from the total number of generated photons with the same parameters as before, we estimate the purely mechanical photon production to be 5×10^{-9} photons/s. Therefore, only one in every million generated photons can be ascribed to mechanical motion alone. However, in our situation it is not possible to experimentally distinguish the photons generated by changes in the electrical boundary conditions from the ones generated by changes in the mechanical boundary conditions. Consequently, we can only talk about electro-mechanically produced photons.

Improving the quality factor of the FBAR will drastically change the picture. Assuming a quality factor of $3 \cdot 10^6$, i.e. 4 orders of magnitude larger, and a smaller $V_{pp} = 5 \mu\text{V}$ results in $\Delta x = 8.5 \cdot 10^{-11}$ m. This high-Q regime is in principle already experimentally accessible with other materials, for example with GHz mechanical oscillators made of silicon [22]. The higher mechanical quality factor and the lower driving voltage benefit the ratio of DCE photons generated via mechanical compared to electrical origin, such that both can be of equal magnitude, see Fig. 3.

Discussion.—Further improvements could be obtained by using a material with higher piezoelectric coefficient, me-

chanical quality factor and dielectric constant for the FBAR. The most promising approach is the use of SQUID-based metamaterials for the resonator. Indeed, recent experiments with metamaterials based on long arrays of Josephson junctions have demonstrated [23, 24] an increase in the effective impedance Z_0 by two orders of magnitude $Z_0 \approx 10^4$ Ohm. This was achieved while keeping the total capacitance of the resonator approximately constant, which means that the speed of light in the metamaterial $v = (CZ_0)^{-1}$ is reduced by two orders of magnitude. Such a device would lead to an enhancement in photon production by four orders of magnitude, from which we can again roughly estimate the ratio of the mechanically produced photons with respect to the electrically generated ones, which would improve by two orders of magnitude. This results from the former scaling with Z_0 , as shown in Eq. (4), while the latter scaling as $Z_0^{1/2}$, as shown in Eq. (5). However, using superconducting metamaterials could lead to other unwanted effects such as the emergence of a finite-size lattice structure or the impedance mismatch between the resonator and the transmission line. Incorporating these properly into our proposal would require more detailed studies, which we leave as a future direction.

Finally, we would like to highlight that there are other traces of the Casimir effect related to quantum correlation functions. For instance, techniques developed in recent accurate experiments to measure two-time correlation functions in propagating quantum microwaves [25, 26] can be used to measure $g^{(2)}(\tau)$. Indeed, the photons which leak out of the cavity will show a decaying behavior of these auto-correlations, however the formalism developed in this letter is not suitable to calculate such effects, as we treat both the capacitor and the voltage source as classical elements.

In summary, we have proposed an experiment consisting of a mechanical resonator based on a FBAR directly coupled to a superconducting cavity, which generates a resonance enhancement of the electro-mechanically generated dynamical Casimir radiation. We calculate the stable flux of photons proceeding from an electro-mechanically amplified quantum vacuum, demonstrating that measuring an effect is within reach of current technology. We also propose a heuristic method to estimate the fraction which can be ascribed to the non-adiabatic change in the mechanical boundary conditions. Further improvements can either be realized by using Josephson metamaterials or a larger mechanical quality factor to enhance both the photon production and the ratio of the purely mechanically generated photons. Our work also paves the way towards experimentally tests of other fundamental relativistic effects, such as the Unruh effect or the Hawking radiation, by properly modifying the appealing proposals in Ref. [14] employing mechanical resonators.

ACKNOWLEDGMENTS

We would like to thank Adrian Parra, Simone Felicetti, Philipp Schmidt, Hans Huebl, Nicola Roch, and Gary Steele for fruitful discussions and useful insights. M.S. and E.S. are grateful for funding through the Spanish MINECO/FEDER

FIS2015-69983-P and Basque Government IT986-16. S.G. acknowledges financial support from Foundation for Fundamental Research on Matter (FOM) Projectruimte grants (15PR3210, 16PR1054), the European Research Council (ERC StG Strong-Q), and the Netherlands Organisation for Scientific Research (NWO/OCW), as part of the Frontiers of Nanoscience program, as well as through a Vidi grant (016.159.369). W.W. acknowledges financial support by Chalmers Area of Advance Nanoscience and Nanotechnology.

Appendix A: Piezoelectromechanical coupling

We base our proposal on an FBAR device of thickness t and square surface area $A = b^2$ with volume $V = A \cdot t$ and define the z -direction (subscript 3) along the thickness of the FBAR. A voltage is applied to the plates of the FBAR, resulting in an electric field along the z -direction that is assumed to be homogeneous. Due to piezoelectric coupling this voltage results in mechanical strain ϵ :

$$\epsilon_{3j} = -d_{3j}E_3 = -d_{3j}\frac{V_3}{t}, \quad (\text{A1})$$

where d_{ij} is the piezoelectric coupling coefficient. This mechanical strain has a geometric and stress-related effect, which are discussed in the following.

1. Geometric effect

Strain leads to contraction or expansion of the mechanical device and, thus, its dimensions change. For the z direction, one obtains:

$$\Delta z = \epsilon_{33} \cdot t = -d_{33}V_3. \quad (\text{A2})$$

This dimensional change shifts the resonance frequency of the FBAR device. Using $\Omega = 2\pi v/2t$ (v velocity of sound) as approximate formula for the resonance frequency of an FBAR, one gets $\Delta\Omega/\Omega_0 = -\Delta t/t \approx -\epsilon_{33}$. Using (A1), one arrives at

$$\frac{\Delta\Omega}{\Omega_0} = d_{33}\frac{V_3}{t}. \quad (\text{A3})$$

2. Stress-related effect

Mechanical strain ϵ results in mechanical stress σ via the relation $\sigma = E\epsilon$ (E is Young's modulus). Mechanical stress over an area A results in a force F acting on the crystal surface $F = \int_A \sigma dA$.

This force can change the resonance frequency of the device, if the crystal structure could not relax along that direction. For example, this would be the case for a doubly, clamped mechanical beam. However, the FBAR has no fixed/clamped boundaries along the z -direction and, thus, can

relax. Hence, we can neglect any shift in resonance frequency of the FBAR.

The force F can result in mechanical driving of the resonator as it acts as an additional source term in its dynamic equation. The solution of a driven, damped harmonic oscillator in Fourier space is

$$\tilde{x}(\omega) = \chi(\omega) \cdot \tilde{F}(\omega)/m, \quad (\text{A4})$$

with the mechanical susceptibility $\chi(\omega) = (\omega_0^2 - \omega^2 - i\gamma\omega)^{-1}$ and the mass m of the resonator. A sinusoidal driving voltage $V_3(t) = V_{pp} \cos(\omega t + \phi)$ results in a force

$$\begin{aligned} F_3(t) &= \int_A \sigma_3(t) dA = Ed_{33} \frac{V_3(t)}{t} \int_A dA \\ &= Ed_{33} \frac{V}{t^2} V_3(t). \end{aligned} \quad (\text{A5})$$

Evaluating the mechanical response $\tilde{x}(\omega)$ on resonance $\omega = \Omega$ yields

$$|\tilde{x}(\Omega)| = \frac{Q}{\Omega^2} \frac{E}{\rho t} d_{33} \frac{V_{pp}}{t}. \quad (\text{A6})$$

This formula can be rewritten by using the FBARs resonance frequency $\Omega = 2\pi v/2t$ (with velocity of sound $v = \sqrt{K/\rho}$, bulk modulus $K = E/(3(1-2\nu))$ and Poisson's ratio ν) to

$$\begin{aligned} |\tilde{x}(\Omega)| &= \frac{Q}{\pi^2} (3(1-2\nu)) d_{33} V_{pp} \\ &= \frac{Q}{\pi^2} (3(1-2\nu)) \Delta z. \end{aligned} \quad (\text{A7})$$

This means that the driven response is by a factor of $\sim Q/\pi^2$ larger than the geometric response Δz alone.

Appendix B: Proposed implementation and modelling

1. FBAR

We base our proposal on existing technology and employ experimental parameters from Ref. [15]. The mechanical resonator is a piezoelectric FBAR, made up of a heterostructure from Al-AIN-Al, whereby the Al is used to contact the piezoelectric AIN. A specific device could have a total thickness of approximately 1000 nm, consisting of a 300 nm SiO₂ layer, two 150 nm Al electrodes surrounding a 350 nm AIN film, with a speed of sound of $v_s = 9100$ m/s. The device could be fabricated on a high-resistivity silicon-on-insulator wafer. We drive the FBAR with an AC voltage source $V(t) = V_{pp} \cos(\Omega t + \phi)$, with $V_{pp} = 0.5$ mV, a driving frequency equal to the fundamental mechanical frequency Ω , and a phase difference $\phi = \frac{\pi}{2}$.

2. Modified Butterworth-Van Dyke circuit

The Modified Butterworth-Van Dyke circuit (MBVD) enables to extract the necessary parameters for modeling a mechanical resonator as an equivalent electrical circuit. This has

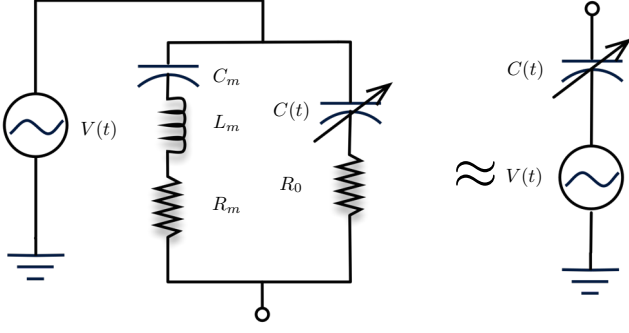


FIG. 4. Equivalent circuit for the FBAR. We have employed the modified van Dyke-Butterworth model to provide the equivalent lumped-element circuit representation of the FBAR.

been, e.g., used in Ref. [15] for calculating the response of the FBAR made from Al/AlN/Al. Note that the MBVD is an approximation of the Generalized Butterworth-Van Dyke circuit for low electro-mechanical coupling k_t^2 .

Reference [30] is used for the following description of the MBVD. Note that Ref. [31] gives a derivation of the more general GBVD modelling acoustic loss, dielectric loss and electrode electrical loss. The simplest model for a FBAR is derived from approximating the 3-port Mason model to a 4 element circuit consisting of a plate capacitance C_0 in parallel with a series $R_m - L_m - C_m$ circuit. This circuit has a series resonance ω_s (given by L_m, C_m as $\omega_s = 1/\sqrt{L_m C_m}$) and a parallel resonance ω_p (set by C_0 in series with L_m, C_m as $(\omega_p/\omega_s)^2 = 1 + 1/r$). The capacitance ratio r is defined as $r = C_0/C_m$.

Adding a series resistor R_s at the input to this model allows to account for the electrode electrical loss. This is the so-called Butterworth-Van Dyke circuit, which has 5 parameters: C_0, R_s, R_m, L_m, C_m . The electro-acoustic coupling constant k_t^2 can be derived to be

$$(k_t)^2 = \frac{\pi^2 \omega_s \omega_p - \omega_s}{4 \omega_p \omega_p} = \frac{\pi^2}{8} \frac{1}{r} \left(1 - \frac{1}{r}\right) \quad (\text{B1})$$

One can add a sixth parameter, a resistor R_0 in series with C_0 , accounting for material loss. This capacitance C_0 actually changes in time when an AC driving is applied, due to the change in the geometric structure. In Ref. [30], it is derived a set of equations to obtain the 6 parameters from measurable quantities: series and shunt resonant frequencies, the effective quality factors Q_{s0}, Q_{p0} , and the capacitance and resistance far away from the resonances.

To model the FBAR we use the experimental parameters from Ref. [15]: $C_m = 0.655$ fF, $L_m = 1.043$ μ H and $R_m = 146$ Ohm for the mechanical part, and $C_0 = 0.19$ pF (average value in time) and $R_0 = 8$ Ohm for the geometric part. We would like to note that a similar FBAR was recently demonstrated with $C_0 = 1.00$ pF [18]. Taking into account that the permittivity of AlN is $\epsilon_{\text{AlN}} \approx 9.2\epsilon_0 = 81$ pF/m and that the distance between the plates is $t_{\text{AlN}} = 330$ nm, we can model a parallel plate capacitor and estimate its area $A = \frac{t_{\text{AlN}} C_0}{\epsilon} \approx 7.7 \cdot 10^{-10}$ m².

In this work, we are primarily interested in calculating the DCE photon production. Therefore, we simplify the full model to the elements containing the most relevant information, as shown in Fig. 4. Taking the parameters considered in Appendix C, then $Z_m = R_m + j(\Omega L_m - \frac{1}{\Omega C_m}) \approx 146 + j2.8 \cdot 10^4$ Ohm, while $Z_0 = R_0 - j\frac{1}{\Omega C_0} \approx 8 - j189$ Ohm. As $Z_{eq} = \frac{Z_0 Z_m}{Z_0 + Z_m} \approx Z_0$, since $|Z_0| \ll |Z_m|$ and the resistor is much smaller than the capacitor, then our approximation follows.

3. Superconducting cavity

The superconducting cavity has a length of $d = 3.3 \cdot 10^{-2}$ m, with a fundamental frequency of $\omega_{c,0} = 2\pi \cdot v/d = 2\pi \cdot 3.03$ GHz with the speed of light in the superconducting material of $v = 10^8$ m/s. It is capacitively coupled to a semi-infinite transmission line with impedance $Z_0 \approx 55$ Ohm. The capacitor coupling the resonator to the transmission line has a frequency $\omega_c/2\pi = (2\pi Z_0 C_c)^{-1} = 7\Omega \approx 2\pi 29.1$ GHz.

Appendix C: Parameters for the proposed implementation

Material properties AlN	
Youngs modulus	$E = 308$ GPa
density	$\rho = 3230$ kg/m ³
piezoelectric coupling	$d_{33} = 5.1 \cdot 10^{-12}$ m/V [28, 29]
Poissons ratio	$\nu = 0.287$ along {0001}
average velocity of sound	$v = 9100$ m/s [15]
permittivity	$\epsilon_{\text{AlN}} \approx 9.2\epsilon_0 = 81$ pF/m
FBAR parameters	
quality factor	$Q = 300$
resonance frequency	$\Omega = 2\pi \cdot 4.2$ GHz
thickness AlN layer	$t_{\text{AlN}} = 350$ nm
total thickness	$t = 950$ nm
drive voltage	$V_{\text{pp}} = 0.5$ mV
driven motional amplitude	$\Delta x(V) = 1.7$ nm/V
Superconducting cavity parameters	
length	$d = 3.3 \cdot 10^{-2}$ m
fundamental frequency	cavity $\omega_{c,0} = 2\pi \cdot 3.03$ GHz
impedance	$Z_0 = 55$ Ohm
DCE capacitance	$C_0 = 0.4 \cdot 10^{-12}$ F
transmission line coupling capacitance	$2\pi \cdot 29.1$ GHz
Further parameters	
Temperature	$T = 10$ mK

This table summarizes the experimental parameters used in this proposal.

-
- [1] M. E. Peskin and D. V. Schroeder, *An Introduction to Quantum Field Theory* (Westview Press, 1995).
- [2] M. Di Ventra, *Electrical Transport in Nanoscale Systems* (Cambridge Univ. Press, 2008).
- [3] W. E. Lamb and R. C. Retherford, *Fine Structure of the Hydrogen Atom by a Microwave Method*, Phys. Rev. **72**, 241 (1947).
- [4] H. B. G. Casimir, *On the attraction between two perfectly conducting plates*, Proc. K. Ned. Akad. Wet. B **51**, 793 (1948).
- [5] S. K. Lamoreaux, *Demonstration of the Casimir Force in the 0.6 to 6 μm Range*, Phys. Rev. Lett. **78**, 5 (1997).
- [6] U. Mohideen and A. Roy, *Precision Measurement of the Casimir Force from 0.1 to 0.9 μm* , Phys. Rev. Lett. **81**, 4549 (1998).
- [7] G. T. Moore, *Quantum Theory of the Electromagnetic Field in a Variable Length One Dimensional Cavity*, J. Math. Phys. **11**, 2679 (1970).
- [8] C. M. Wilson, G. Johansson, A. Pourkabirian, M. Simoen, J.R. Johansson, T. Duty, F. Nori and P. Delsing, *Observation of the dynamical Casimir effect in a superconducting circuit*, Nature **479**, 376 (2011).
- [9] P. Lähteenmäki, G. S. Paraoanu, J. Hassel, and P. J. Hakonen, *Dynamical Casimir effect in a Josephson metamaterial*, Proc. Natl. Acad. Sci. U.S.A. **110**, 4234 (2013).
- [10] S. Felicetti, M. Sanz, L. Lamata, G. Romero, G. Johansson, P. Delsing, and E. Solano, *Dynamical Casimir Effect Entangles Artificial Atoms*, Phys. Rev. Lett. **113**, 093602 (2014).
- [11] D. Z. Rossatto, S. Felicetti, H. Eneriz, E. Rico, M. Sanz, and E. Solano, *Entangling polaritons via dynamical Casimir effect in circuit quantum electrodynamics*, Phys. Rev. B **93**, 094514 (2016).
- [12] J. R. Johansson, G. Johansson, C. M. Wilson, and F. Nori, *Dynamical Casimir effect in superconducting microwave circuits*, Phys. Rev. A **82**, 052509 (2010).
- [13] A. Lambrecht, M. T. Jaekel, and S. Reynaud, *Motion induced radiation from a vibrating cavity*, Phys. Rev. Lett. **77**, 615 (1996).
- [14] P. D. Nation, J. R. Johansson, M. P. Blencowe, and F. Nori, *Stimulating uncertainty: Amplifying the quantum vacuum with superconducting circuits*, Rev. Mod. Phys. **84**, 1 (2012).
- [15] A. D. O'Connell, et al. *Quantum ground state and single-phonon control of a mechanical resonator*, Nature **464**, 697 (2010).
- [16] J. D. Larson III, P. D. Bradley, S. Wartenberg, and R. C. Ruby in Proc. 2000 IEEE Ultrasonics Symp. (IEEE, 2000).
- [17] K. Nam, et al., *Piezoelectric properties of aluminium nitride for thin film bulk acoustic wave resonator*, J. Korean Phys. Soc. **47**, 309 (2005).
- [18] P. R. Reddy and B. C. Mohan, *Design and Analysis of Film Bulk Acoustic Resonator (FBAR) Filter for RF Applications*, Int. J. Eng. Bus. Manag. **4**, 29 (2012).
- [19] K. G. Fedorov et al., *Finite-time quantum correlations of propagating squeezed microwaves*, ArXiv preprint: 1703.05138 (2017).
- [20] E. P. Menzel et al., *Dual-Path State Reconstruction Scheme for Propagating Quantum Microwaves and Detector Noise Tomography*, Phys. Rev. Lett. **105**, 100401 (2010).
- [21] R. Di Candia et al., *Dual-path methods for propagating quantum microwaves*, New J. Phys. **16**, 015001 (2014).
- [22] S. M. Meenehan, J. D. Cohen, S. Gröblacher et al., *Silicon optomechanical crystal resonator at millikelvin temperatures*, Phys. Rev. A **90**, 011803(R) (2014).
- [23] N. A. Masluk, I. M. Pop, A. Kamal, Z. K. Mineev, M. H. Devoret, *Microwave characterization of Josephson junction arrays: implementing a low loss superinductance* Phys. Rev. Lett. **109**, 137002 (2012).
- [24] T. Weissl, B. Kueng, E. Dumur, A. K. Feofanov, I. Matei, C. Naud, O. Buisson, F. W. J. Hekking, and W. Guichard, *Kerr coefficients of plasma resonances in Josephson junction chains* Phys. Rev. B **92**, 104508 (2015).
- [25] K. G. Fedorov et al, *Displacement of propagating squeezed microwave states*, Phys. Rev. Lett. **117**, 020502 (2016).
- [26] K. G. Fedorov et al. *Finite-time quantum entanglement in propagating squeezed microwaves*, ArXiv: 1703.05138 (2017).
- [27] R. Di Candia et al, *Quantum teleportation of propagating quantum microwaves*, EPJ Quantum Technology **2**, 25 (2015).
- [28] C. M. Lueng, H. L. W. Chan, C. Surya, and C. L. Choy, *Piezoelectric coefficient of aluminum nitride and gallium nitride*, Journal of Applied Physics **88**, 5360 (2000).
- [29] M.-A. Dubois and P. Muralt, *Properties of aluminum nitride thin films for piezoelectric transducers and microwave filter applications*, Appl. Phys. Lett. **74**, 3032 (1999).
- [30] J. D. Larson, P. D. Bradley, S. Wartenberg, and R. C. Ruby, *Modified Butterworth–Van Dyke circuit for FBAR resonators and automated measurement system*, Proceedings of the IEEE Ultrasonics Symposium **1**, 863 (2000).
- [31] H. Jin, S. R. Dong, J. K. Luo, and W. I. Milne, *Generalised Butterworth–Van Dyke equivalent circuit for thin-film bulk acoustic resonator*, Electronic Letters **47**, 424 (2011).